

Control volume method for hydro-magnetic dynamos in non-uniformly stratified spherical shells

J. Šimkanin

Institute of Geophysics, Academy of Sciences of CR¹

Abstract: The numerical modelling of hydromagnetic dynamos in a rotating spherical shell using the control volume method is presented. The influence of non-uniform stratification and viscosity on hydromagnetic dynamo action has been investigated. The results indicate that the influence of non-uniform stratification of a spherical shell on hydromagnetic dynamos in the present geometric configuration is noticeable. Convection is columnar and runs in both stably and unstably stratified sublayers, although it is slightly suppressed in the stably stratified region. The generated magnetic fields are mostly dipole dominated. Temperature, pressure, velocity and magnetic fields are significantly modified mainly close to the outer boundary.

Key words: hydromagnetic dynamos, control volume method, non-uniform stratification of spherical shells

1. Introduction

Magnetic fields in the universe are most probably generated by hydro-magnetic dynamos. The geomagnetic field is similarly generated by the hydromagnetic dynamo (Geodynamo), which acts in the outer liquid Earth's core. Numerical modelling of self-consistent dynamos has made noticeable progress in the last decade due to the progress in computer technology (for more details, see, e.g., *Roberts and Glatzmaier, 2000*). Its results are in very good agreement with the observations of the recent geomagnetic field and with paleomagnetic research (*Kono and Roberts, 2002*). In most cases, thermal magnetoconvection constitutes the driving mechanism of the dynamos (see, e.g., *Jones, 2000* and *Roberts and Glatzmaier, 2000*). In spite of the huge amount of physical models, almost all of them are based on the same

¹ Boční II/1401, 141 31 Prague, Czech Republic; e-mail: jano@ig.cas.cz

numerical method, namely the spectral method. As stated above, the numerical results agree with observations. However, numerical simulations of the geomagnetic field are not able to run in an Earth-like parameter regime because of the considerable spatial resolution that is required (*Glatzmaier, 2002*). At some resolution, grid methods could be more efficient on parallel computer architectures because only the “nearest neighbour” communication between the processors would be needed – instead of the global communication necessary for spherical harmonic codes (see *Glatzmaier, 2002* and *Hejda and Reshetnyak, 2004*). The control volume method (*Patankar, 1980*) is one of the local methods which would be available for dynamo simulations, and which achieves a given accuracy at high resolutions.

The control volume method was successfully used for self-consistent dynamo simulations (*Hejda and Reshetnyak, 2003* and *Harder and Hansen, 2005*) and tested on the standard solution (the dynamo benchmark) for convection (*Hejda and Reshetnyak, 2004*). In the present paper an attention is focused on the study of hydromagnetic dynamos in non-uniformly stratified spherical shells. The outer liquid Earth’s core and the liquid interiors of Giant planets are namely non-uniformly stratified. The non-uniform stratification (this means density stratification) results from the complicated processes going on in their interiors. For example, the non-uniform stratification of the outer Earth’s core (*Fearn and Loper, 1981*; *Šimkanin et al., 2003* and *Šimkanin et al., 2006*) is due to chemical homogenisation, gravitational differentiation, solidification processes acting on the inner core boundary (e.g., the convection in the mushy layer due to the mentioned solidification processes, see *Guba and Worster, 2006*), etc. These processes are also the basic sources of the buoyancy, which constitutes the fundamental source of (magneto)convection and hydromagnetic dynamos (see, e.g., *Jones, 2000* or *Velímský and Matyska, 2000*).

It is assumed that the upper part of the outer liquid Earth’s core (close to the core-mantle boundary²) is stably stratified (subadiabatic radial temperature gradient) and the lower part (towards the inner core boundary³) unstably (superadiabatic radial temperature gradient). The stably stratified sublayer is probably very thin (for more details related to the the non-uniform stratification of the outer Earth’s core, see, e.g., *Fearn and Loper, 1981*;

² hereinafter referred to as CMB

³ hereinafter referred to as ICB

Šimkanin et al., 2003 and *Šimkanin et al., 2006*). The models of the non-uniformly stratified fluid shell (and also horizontal layer) are an acceptable simplification of the real Earth-like conditions. The results of previous analyses have shown that the hydromagnetic systems are strongly affected by non-uniform stratification, electromagnetic properties of the boundaries, diffusive processes (the complicated coupling of viscous, thermal and magnetic processes) and the dynamical coupling of magnetic (Lorentz), Archimedean and Coriolis forces (*Šimkanin et al., 2003* and *Šimkanin et al., 2006*).

The model and governing equations are given in Section 2. The numerical results are presented in Section 3. Finally, Section 4 provides the conclusions.

2. Governing equations

The generation of magnetic field \mathbf{B} by incompressible flow \mathbf{V} in the Boussinesq approximation in a spherical shell ($r_i < r < r_0$) rotating with angular velocity Ω is described by the system of dimensionless equations:

$$\frac{\partial \mathbf{B}}{\partial t} = \nabla \times (\mathbf{V} \times \mathbf{B}) + q^{-1} \nabla^2 \mathbf{B}, \quad (1)$$

$$P_r^{-1} E \left(\frac{\partial \mathbf{V}}{\partial t} + (\mathbf{V} \cdot \nabla) \mathbf{V} \right) = -\nabla P - \mathbf{1}_z \times \mathbf{V} + R_a T r \mathbf{1}_r + (\nabla \times \mathbf{B}) \times \mathbf{B} + E \nabla^2 \mathbf{V}, \quad (2)$$

$$\frac{\partial T}{\partial t} + (\mathbf{V} \cdot \nabla) T = \nabla^2 T + G, \quad (3)$$

$$\nabla \cdot \mathbf{V} = 0, \quad \nabla \cdot \mathbf{B} = 0. \quad (4)$$

The typical length scale is the radius of sphere L , which makes the dimensionless radius $r_0 = 1$; the inner core radius r_i is, similarly to that of the Earth, equal to 0.35. (r, θ, φ) is the spherical system of coordinates, $\mathbf{1}_z$ and $\mathbf{1}_r$ are the unit vectors. The typical diffusion time, t , velocity, \mathbf{V} , magnetic field, \mathbf{B} , and pressure, P , are then measured in units of L^2/κ , κ/L , $\sqrt{2\Omega\kappa\mu\rho}$, $\rho\kappa^2/L^2$, respectively. The dimensionless parameters appearing in (1-4) are the Roberts number $q = \kappa/\eta$, the Prandtl number

$P_r = \nu/\kappa$, the Ekman number $E = \nu/2\Omega L^2$ and the modified Rayleigh number $R_a = \alpha g_0 \delta T L / 2\Omega \kappa$, where κ is thermal diffusivity, η is magnetic diffusivity, ν is kinematic viscosity, μ is permeability, ρ is density, α is the coefficient of volume expansion, δT is the drop of temperature through the shell and g_0 is the gravity acceleration at $r = r_0$.

The inner core ($r \leq r_i$) with surface S can rotate about the axis of rotation due to the viscous and magnetic torque τ . The evolution of the angular velocity ω of the inner core is described by the following momentum equation

$$EI \frac{\partial \omega}{\partial t} = P_r r_i \oint_S \tau_{r\varphi} \Big|_{r=r_i} \sin \theta \, dS, \quad (5)$$

where I is the moment of inertia of the inner core and τ_{ij} is the stress-tensor given by the sum of the viscous and Maxwell stresses

$$\tau_{r\varphi} = E \left(\frac{\partial V_\varphi}{\partial r} + \frac{1}{r \sin \theta} \frac{\partial V_r}{\partial \varphi} - \frac{V_\varphi}{r} \right) + B_r B_\varphi \sin \theta.$$

The last term in Eq. (3), $G(r)$, constitutes the heat sources. It enables to simulate various stratifications of the spherical shell. The outer core was assumed to be stratified non-uniformly (the shell is divided into stably and unstably stratified sub-shells) with constant temperature $T_i = 1$ and $T_0 = 0$ at the inner and outer boundaries of the shell (as traditionally in dynamo simulations). Thus, the non-uniform stratification was considered by heat sources in the form:

$$G(r) = (9rr_{ICB}^2 - 12r + 6r^2r_{ICB}^2 + 60r^2 - 2r_{ICB}^2 - 8 + r_{ICB}^4 - 12r_{ICB}r^2 - 6rr_{ICB}^3 - 18r_{ICB}r) / [r(r_{ICB}^2 - 4)]. \quad (6)$$

$\frac{\partial T}{\partial r}$ changes its sign in the middle of the convective shell, $r_m = (r_{ICB} + r_{CMB})/2$ (for more details, see *Reshetnyak and Steffen, 2005*).

Eqs (1-4) are closed by the non-penetrating and no-slip boundary conditions for the velocity field at the rigid surfaces, zero boundary conditions for temperature perturbations T and vacuum boundary conditions for the magnetic field. The conductivity of the inner core is assumed to be the same as that of the liquid part.

3. Numerical results

Eqs (1-4) were solved using the control volume method (for more details see, e.g., *Hejda and Reshetnyak, 2003*). It is assumed that all fields are defined at the nodes which are the centres of grid cells (control volumes). The basic strategy of the method is to express the differential equations in conservative form, integrate them over the control volumes and convert every such integral into the sum of fluxes over the boundary faces by means of Gauss' theorem. It is advantageous to employ a different grid for each component of the vector fields (and an additional grid for the scalar field). Then, if we consider, e.g., the heat flux equation, the velocity components are calculated for the points that lie on the corresponding faces of the control volumes. The discrete form of the system of linear equations is represented by the band matrix. Note that it is the flux form of the equations which allows us to omit the boundary conditions at the axis (and at the centre of the sphere if the magnetic field is taken into account) because the flux is zero at the faces with zero area. Nevertheless, extrapolation to the axis is necessary in some situations. It is well known that convection-diffusion problems are prone to instabilities for larger Reynolds numbers. Whereas the simplest remedy for this difficulty is the up-wind scheme, the power-law scheme of second-order accuracy has been used. The linear system of equations was solved using the tridiagonal solver in the r -direction and the Gauss-Seidel iterative algorithm with underrelaxation in the tangential directions (*Patankar, 1980*).

Our control volume code was verified on the so-called numerical dynamo benchmark (see *Christensen et al., 2001*). Case 0 (the thermal convection in a rotating spherical shell) has been successfully tested and already presented (see *Hejda and Reshetnyak, 2004*) and Case 2 (the dynamo with conducting and rotating inner core) is also in agreement with it. The solution of the dynamo benchmark is quasi-stationary, drifting slowly in longitude, symmetric about the equator (dipole parity) and has fourfold symmetry in longitude. Convection is columnar and the magnetic field at the outer boundary is strongly dipolar and dominated by four flux lobes (*Christensen et al., 2001*).

Parallelization is carried out using the message-passing interface (MPI). The computations were performed on an IBM Regatta p690+ cluster of SMP

nodes in the John von Neumann Institute for Computing, Jülich Research Centre; SunFire V890 at the Institute of Physics, Academy of Sciences, Prague and PC clusters.

As stated above, the outer Earth's core is probably non-uniformly stratified (due to thermodynamic processes acting therein), i.e. it is divided into two sublayers (see *Fearn and Loper, 1981* and *Šimkanin et al., 2006*). The upper sublayer (close to CMB) is stably stratified ($\frac{\partial T}{\partial r} > 0$) and the lower one (close to ICB) unstably ($\frac{\partial T}{\partial r} < 0$). In the Earth's core the stably stratified sublayer is probably very thin (the outer Earth's core is almost unstably stratified). However, in the other planets the ratio of the thickness of the appropriate sublayers (e.g., of the stably stratified to unstably stratified sublayers) and the geometric configuration vary (see *Zhang and Schubert, 2000*, *Stanley and Bloxham, 2006* and *Christensen, 2006*). This is noticeable especially with the Giant planets (for more details, see, e.g., *Stanley and Bloxham, 2004*, *Stanley and Bloxham, 2006* and *Zhang and Schubert, 2000*). Non-uniform stratification can be simulated thermodynamically also in the Boussinesq models by means of internal heat sources (for more details, see *Šimkanin et al., 2003* and *Šimkanin et al., 2006*). If the stably stratified sublayer is very thin (for a geometric configuration stable/unstable), it is very similar to the case of uniform stratification when the whole layer is unstably stratified. However, the effects of non-uniform stratification are noticeable when the thickness of the stably and unstably stratified sublayers is comparable (see *Šimkanin et al., 2003* and *Šimkanin et al., 2006*). Consequently, the change of the sign was located to the middle of the convective shell (the thickness of both sublayers is the same).

The influence of non-uniform stratification on a hydromagnetic dynamo (Geodynamo) action was studied for parameters $R_a = 550$, $P_r = 1$ and various values of the Ekman, E , and Roberts, q , numbers (see Table 1). The forward integration of the equations was possible only with a very small time step of (from 10^{-6} to 10^{-7}), even for higher values of the Ekman number. Consequently, computations had high demands on the computer time. The spatial resolution was $85 \times 85 \times 160$ ($K_r \times K_\theta \times K_\varphi$), where K_r , K_θ , K_φ are the numbers of grid points in the appropriate directions r , θ , φ , respectively. The monitored output parameters are the mean kinetic energy, E_k , the mean magnetic energy in the shell, E_m , and in the inner core, E_m^{ic} , the mean angular drift of the solution, ω , and the mean angular frequency of

differential rotation of the inner core, ω_{ic} . The results (dependence of the monitored output parameters on the Ekman number, E , and the Roberts number, q) are summarized in Table 1. The typical space distribution of pressure and temperature for the case with $E = 10^{-4}$ and $q = 2$ (the lowest used value of the Ekman number) are presented in Fig. 1, and of the velocity and magnetic fields in Figs 2 and 3, respectively. All cases (presented in Table 1) are characterized by columnar convection, solution of fourfold symmetry in longitude and the magnetic field which is dominated by four flux lobes. Fig. 2 (the space distribution of the velocity field) presents a typical example of the multilayer convection mode. The convection runs in both the stably and unstably stratified sublayers, although it is slightly suppressed in the stably stratified region and shifted away from the CMB (Fig. 2). Namely, the positive temperature gradient in the stably stratified sublayer suppresses convection in the region close to CMB (see *Zhang and Schubert, 2000*). In the first case ($E = 10^{-1}$ and $q = 8$) the magnetic field at the outer boundary is non-dipolar, in the remaining ones it is dipolar (as assumed). These results are in good agreement with the previous analyses related to systematic parameter studies (but done in the uniformly stratified spherical shell, see, e.g., *Christensen and Aubert, 2006*).

As written above, the case with $E = 10^{-4}$ and $q = 2$ is presented because of the lowest used value of the Ekman number. Fig. 1 shows how significantly the temperature and pressure are influenced by the positive temperature gradient in the stably stratified sublayer (as assumed, especially close to CMB, see Fig. 1). As also assumed, the convection is noticeably influenced by non-uniform stratification especially close to CMB (see Fig. 2), i.e. it is slightly suppressed in the stably stratified region and shifted away from CMB (Fig. 2). In addition, Fig. 2 provides a typical example of the multilayer convection mode. Looking at Fig. 2, it is possible to observe the strong V_φ -component of velocity due to forcing as consequence of a presence of a stably stratified sublayer (for more details, see *Lister, 2004*). Such effect becomes stronger at the low Ekman numbers. The magnetic field is also noticeably modified, mainly at CMB. Looking at Fig. 3 it is possible to observe that the stably stratified sublayer visibly modifies the magnetic field in this region, mainly at CMB, although it remains dipolar. Consequently, it is possible to conclude that the influence of non-uniform stratification on the hydromagnetic dynamo in the present geometric configuration is no-

Table 1. Dependence of the mean kinetic energy, E_k , the mean magnetic energy in the shell, E_m , the mean magnetic energy in the core, E_m^{ic} , the mean drift velocity, ω , and the mean angular frequency of differential rotation of the inner core, ω_{ic} , on the Ekman number, E , and the Roberts number, q

E	q	E_k	E_m	E_m^{ic}	ω	ω_{ic}
10^{-1}	8	805.3	3619	3365	-1.6541	-0.9337
10^{-2}	5	773.6	3403	2722	-1.5342	-0.7962
10^{-3}	5	1459	16049	14922	-1.5913	-0.8527
10^{-4}	2	2318	44042	40950	-1.6443	-0.9116

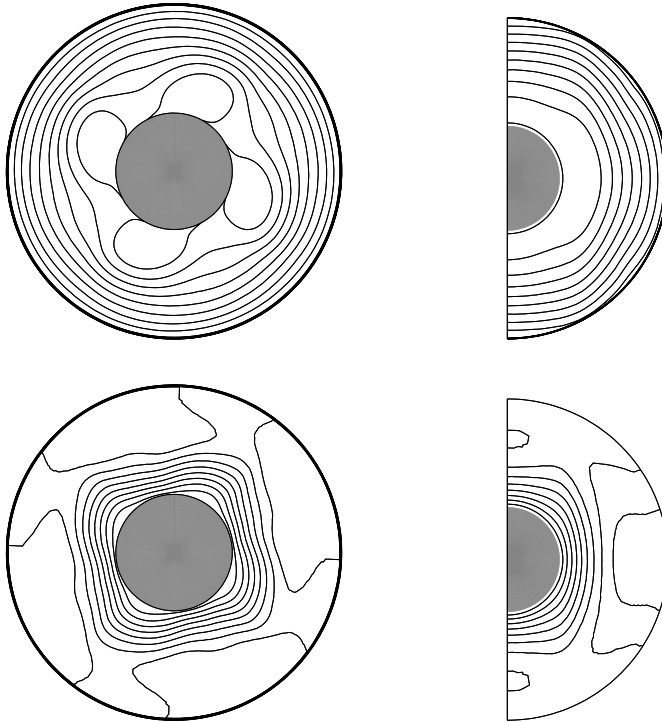


Fig. 1. Pressure, P , (upper line) and temperature, T , (bottom line); equatorial (left column) and axi-symmetrical meridional (right column) sections, for $E = 10^{-4}$ and $q = 2$.

ticeable, which could be considered as typical for the Earth and probably also for the Giant planets such as Jupiter and Saturn. Presented results are certainly influenced also by viscosity (various values of Ekman number) and various measure of thermal and magnetic diffusive processes (various values of Roberts numbers). However, the most dominant effects are of the non-uniform stratification.

Another good example of the influence of stably stratified sublayer provides the study of a hydromagnetic dynamo action in Mercury (*Christensen, 2006*). Mercury is characterized by the weak magnetic field. A possible explanation could be given by a hydromagnetic dynamo working in the similar geometric configuration as at our study (stable/unstable) but in this case more part of spherical shell is stably stratified (*Christensen, 2006*). In such case the (magneto)convection (see *Šimkanin et al., 2003* and *Zhang and Schubert, 2000*) and dynamo action (*Christensen, 2006*) are strongly suppressed in the upper stably stratified sublayer (the most part of shell is stably stratified), i.e. magneto(convection) and dynamo run in the small unstably stratified sublayer (close to ICB). Consequently, a magneto(convection) is weak (*Šimkanin et al., 2003* and *Zhang and Schubert, 2000*). Such weak dynamo action and skin-effect (the magnetic field generated in the unstably stratified sublayer permeates through the stably stratified sublayer where is damped due to skin-effect) lead to the weak magnetic field observed on the surface of Mercury (*Christensen, 2006*).

For a different geometric configuration this influence can be much stronger (see, e.g., *Stanley and Bloxham, 2004 and 2006*). Having assumed reverse stratification, i.e. the stably stratified sublayer is surrounded by the unstably stratified one, the given configuration leads to non-dipolar and non-axisymmetric magnetic fields, which are typical for instance for Uranus and Neptune. A similar effect can be achieved if different electromagnetic boundary conditions are considered for the outer (CMB) and inner (ICB) boundaries, e.g., the electrical conductivity of CMB is much greater than that of ICB (*Stanley and Bloxham, 2004*). The dependence of the hydromagnetic dynamo (mainly Geodynamo) on electromagnetic boundary conditions of CMB and ICB is described very well by *Wicht (2002)*.

Let us briefly comment the efficiency of our numerical code. The lowest used value of the Ekman number is $E = 10^{-4}$ because the value $E = 10^{-6}$ constitutes the strong limitation of our dynamo code. From this point of

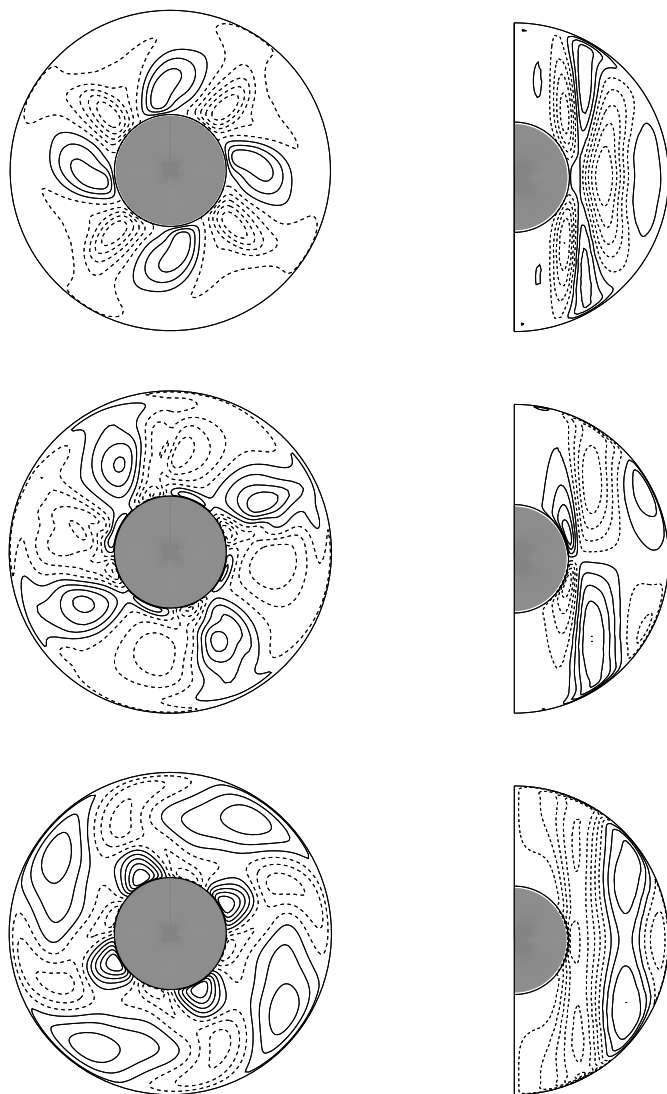


Fig. 2. Velocity field components (V_r , V_θ , V_ϕ) (from top to bottom); equatorial (left column) and axi-symmetrical meridional (right column) sections, for $E = 10^{-4}$ and $q = 2$.



Fig. 3. Magnetic field components (B_r, B_θ, B_φ) (from top to bottom); equatorial (left column) and axi-symmetrical meridional (right column) sections, for $E = 10^{-4}$ and $q = 2$.

view the models presented in *Stanley and Bloxham (2006)* and *Christensen (2006)* are more realistic because the lower Ekman numbers and the greater Rayleigh numbers were used. Having compared our dynamo code based on the control volume method with dynamo codes based on spectral methods, it is possible to conclude that spectral methods are much more effective than our control volume code.

The presented results are in agreement with previous analyses of non-uniform stratification (e.g., the simple test in *Reshetnyak and Steffen, 2005*). The influence of non-uniform stratification on hydromagnetic dynamo action is noticeable. However, it is possible to expect this dependence to be much stronger in the study of turbulence (*Reshetnyak and Steffen, 2005*).

4. Conclusions

The control volume method is an other numerical method available for numerical modelling of a self-consistent dynamo (*Hejda and Reshetnyak, 2003*; *Reshetnyak and Steffen, 2005* and *Harder and Hansen, 2005*). The Case 0 (thermal convection in a rotating spherical shell) has been successfully tested (see *Hejda and Reshetnyak, 2004*) and Case 2 (the dynamo with conducting and rotating inner core) is also in agreement with it. Various dynamo modes were investigated for various input parameters and geometric configurations (for more details, see *Reshetnyak and Steffen, 2005*). The influence of non-uniform stratification on hydromagnetic dynamo action was studied for various values of the Ekman and Roberts numbers (see Table 1). The employed time step had to be very small (from 10^{-6} to 10^{-7}), even for higher values of the Ekman number.

All cases are characterized by columnar convection, solution of fourfold symmetry in longitude and magnetic field which is dominated by four flux lobes. The magnetic field at the outer boundary is dipolar (see Table 1 and Figs 1–3), except for the case with $E = 10^{-1}$ and $q = 8$ when it is non-dipolar. The influence of non-uniform stratification on the hydromagnetic dynamo is noticeable for temperature, pressure, velocity and magnetic fields. They are certainly influenced also by viscosity (various values of Ekman number) and various measure of thermal and magnetic diffusive processes (various values of Roberts numbers). However, the most dominant

effects are of the non-uniform stratification. It is visible mainly close to CMB, where the effects of the stably stratified sublayer are the most significant and strongest, i.e. convection is slightly suppressed in the stably stratified region and shifted away from CMB and the magnetic field is significantly modified, particularly close to CMB. Consequently, it is possible to conclude that the influence of non-uniform stratification on the hydromagnetic dynamo in the present geometric configuration is noticeable which could be considered as typical for the Earth and probably also for the Giant planets such as Jupiter and Saturn (but is not as significantly strong as in *Stanley and Bloxham, 2004* and *Stanley and Bloxham, 2006* where different geometric configuration leads to magnetic fields typical for Uranus and Neptune). However, it is possible to expect that an influence of non-uniform stratification on a hydromagnetic dynamo to be much stronger in the study of turbulence (*Reshetnyak and Steffen, 2005*).

$E = 10^{-4}$ was the lowest used value because $E = 10^{-6}$ constitutes the limitation of our dynamo code (high demands on the computer time). From this point of view the models presented in *Stanley and Bloxham (2006)* and *Christensen (2006)* are more realistic because the lower Ekman numbers and the greater Rayleigh numbers were used. Comparing efficiency of spectral methods with our dynamo code based on control volume method, we are able to conclude that the spectral methods are much more effective than control volume method for dynamo modelling when we investigate the global fields. It is possible to expect that the control volume method will be more effective at local analyses of turbulence (see, e.g., *Reshetnyak and Steffen, 2005*).

Acknowledgments. This research has been supported by the Grant Agency of the Academy of Sciences of the Czech Republic (Grant IAA300120704), the INTAS Foundation (Grant 03-51-5807) and the John von Neumann Institut für Computing, Forschungszentrum Jülich (Grant #k2720000).

References

- Christensen U. R., Aubert J., Cardin P., Dormy E., Gibbons S., Glatzmaier G. A., Grote E., Honkura Y., Jones C., Kono M., Matsushima M., Sakuraba A., Takahashi F., Tilgner A., Wicht J., Zhang K., 2001: A numerical dynamo benchmark. *Phys. Earth Planet. Inter.*, **128**, 25–34.

- Christensen U. R., Aubert J., 2006: Scaling properties of convection-driven dynamos in rotating spherical shells and application to planetary magnetic fields. *Geophys. J. Int.*, **166**, 97–114.
- Christensen U. R., 2006: A deep dynamo generating Mercury's magnetic field. *Nature*, **444**, 1056–1058. doi:10.1038/nature05342
- Fearn D. R., Loper D. E., 1981: Compositional convection and stratification of the Earth's core. *Nature*, **289**, 393–394.
- Glatzmaier G. A., 2002: Geodynamo simulations – how realistic are they? *Annu. Rev. Earth Planet. Sci.*, **30**, 237–257.
- Guba P., Worster M. G., 2006: Nonlinear oscillatory convection in mushy layers. *J. Fluid Mech.*, **553**, 419–443.
- Harder H., Hansen U., 2005: A finite-volume solution method for thermal convection and dynamo problems in spherical shells. *Geophys. J. Int.*, **161**, 522–532.
- Hejda P., Reshetnyak M., 2003: Control volume method for the dynamo problem in the sphere with free rotating inner core. *Studia geoph. et geod.*, **47**, 147–159.
- Hejda P., Reshetnyak M., 2004: Control volume method for the thermal convection problem in a rotating spherical shell: test on the benchmark solution. *Studia geoph. et geod.*, **48**, 741–746.
- Jones C. A., 2000: Convection-driven geodynamo models. *Phil. Trans. R. Soc. Lond. A*, **358**, 873–897.
- Kono M., Roberts P. H., 2002: Recent geodynamo simulations and observations of the geomagnetic field. *Rev. Geophys.*, **40** (4), art. no. 1013.
- Lister J. R., 2004: Thermal winds forced by inhomogeneous boundary conditions in rotating, stratified hydromagnetic fluid. *J. Fluid Mech.*, **505**, 163–178.
- Patankar S. V., 1980: *Numerical Heat Transfer And Fluid Flow*. Taylor and Francis.
- Reshetnyak M., Steffen B., 2005: A dynamo model in a spherical shell. *Numerical Methods And Programming*, **6**, 27–34.
- Roberts P. H., Glatzmaier G. A., 2000: Geodynamo theory and simulations. *Rev. Mod. Phys.*, **72** (4), 1081–1123.
- Stanley S., Bloxham J., 2004: Convective-region geometry as the cause of Uranus' and Neptune's unusual magnetic fields. *Nature*, **428**, 151–153.
- Stanley S., Bloxham J., 2006: Numerical dynamo models of Uranus' and Neptune's magnetic fields. *Icarus*, **184**, 556–572.
- Šimkanin J., Brestenský J., Ševčík S., 2003: Problem of the rotating magnetoconvection in variously stratified fluid layer revisited. *Studia geoph. et geod.*, **47**, 827–845.
- Šimkanin J., Brestenský J., Ševčík S., 2006: On hydromagnetic instabilities and the mean electromotive force in a non-uniformly stratified Earth's core affected by viscosity. *Studia geoph. et geod.*, **50**, 645–661.
- Velínský J., Matyska C., 2000: The influence of adiabatic heating/cooling on magneto-hydrodynamic systems. *Phys. Earth Planet. Inter.*, **117**, 197–207.
- Wicht J., 2002: Inner-core conductivity in numerical dynamo simulations. *Phys. Earth Planet. Inter.*, **132**, 281–302.

Zhang K., Schubert G., 2000: Teleconvection: remotely driven thermal convection in rotating stratified spherical layers. *Science*, **290**, 1944–1947.